Eur Biophys J (2011) 40:947–957
DOI 10.1007/s00249-011-0710-7

ORIGINAL PAPER

Plasma membrane charging of Jurkat cells by nanosecond pulsed electric fields

Jody A. White · Uwe Pliquett · Peter F. Blackmore · Ravindra P. Joshi · Karl H. Schoenbach · Juergen F. Kolb

Received: 12 January 2011 / Revised: 13 April 2011 / Accepted: 28 April 2011 / Published online: 19 May 2011

Abstract The initial effect of nanosecond pulsed electric fields (nsPEFs) on cells is a change of charge distributions along membranes. This first response is observed as a sudden shift in the plasma transmembrane potential that is faster than can be attributed to any physiological event. These immediate, yet transient, effects are only measurable if the diagnostic is faster than the exposure, i.e., on a nanosecond time scale. In this study, we monitored changes in the plasma transmembrane potential of Jurkat cells exposed to nsPEFs of 60 ns and amplitudes from 5 to 90 kV/cm with a temporal resolution of 5 ns by means of the fast voltage-sensitive dye Annine-6. The measurements suggest the contribution of both dipole effects and asymmetric conduction currents across opposite sides of the cell to the charging. With the application of higher field strengths the membrane charges until a threshold voltage value of 1.4–1.6 V is attained at the anodic pole. This indicates when the ion exchange rates exceed charging currents, thus providing strong evidence for pore formation. Prior to reaching this threshold, the time for the charging of the membrane by conductive currents is qualitatively in agreement with accepted models of membrane charging, which predict longer charging times for lower field strengths. The comparison of the data with previous studies suggests that the sub-physiological induced ionic imbalances may trigger other intracellular signaling events leading to dramatic outcomes, such as apoptosis.

Keywords nsPEF · Plasma membrane charging · Membrane poration · Real-time fluorescence imaging · Annine-6

J. A. White · U. Pliquett · K. H. Schoenbach · J. F. Kolb
Frank Reidy Research Center for Bioelectrics,
Old Dominion University, Norfolk, VA, USA

P. F. Blackmore
Department of Physiological Sciences,
Eastern Virginia Medical School, Norfolk, VA, USA

R. P. Joshi · J. F. Kolb (✉)
Department of Electrical and Computer Engineering,
Old Dominion University, Norfolk, VA, USA
e-mail: jkolb@odu.edu

Introduction

With pulsed electric fields of nanosecond duration, it is now possible to instigate specific cell responses, such as apoptosis, release of signaling molecules, progression into the next stage of the cell cycle, etc. (Beebe and Schoenbach 2005; Teissié et al. 2002a). These effects depend on specific pulse parameters, which include pulse shape, duration, rise time, and the intensity (voltage) and number of pulses (frequency). It is proposed that the eventual physiological response is due to the preceding, dramatic, albeit transient, changes in membrane potentials, both extra- and intracellular (Knisley et al. 1993; Krassowska and Neu 1994; Simcic et al. 1997; Joshi et al. 2004). For different exposure parameters different charging mechanisms will be predominant and as a result will allow us to reach different event thresholds (Teissié et al. 2002b). With conventional electroporation pulses of several microseconds and field strengths of only a few hundred volts per centimeter, it is generally believed that only the plasma membrane is affected (Tsong 1991). After reaching a cell-specific threshold, predicted to be on the order of 1 V, the formation of conductive membrane defects in the plasma membrane is anticipated (Tsong 1991). The permeabilization of the membrane is generally ascribed to pores, which reseal

in seconds to minutes after removal of the applied field (Tsong 1991). With fast-rising electric fields of shorter duration, termed nanosecond pulsed electric fields (nsPEFs), sub-cellular structures will also be exposed to the applied field, and for high field strengths their membranes can be charged significantly (Beebe et al. 2004a; Beebe et al. 2004b; White et al. 2004; Scarlett et al. 2009). We believe that reaching different cellular transmembrane voltage thresholds is responsible for the various cell responses observed. These secondary mechanisms after exposure are currently being studied, but as of yet are far from complete. For the induction of apoptosis several studies have already identified pulse parameter thresholds (Beebe et al. 2003; Vernier et al. 2004a). This recently led to the development of a treatment for melanoma that resulted in the arrest and demise of tumors in mice (Nuccitelli et al. 2006).

Whereas the physiological cell responses can be investigated with standard diagnostic techniques such as microscopy, histology, or flow cytometry (Scarlett et al. 2009; Nuccitelli et al. 2006; Vernier et al. 2004b; Beebe et al. 2003), the study of immediate interactions between the pulsed electric fields and cells would require not readily available diagnostics with a temporal resolution that is short compared to the duration of the exposure. As an alternative, mechanisms have been investigated with numerical methods and computer simulations instead. These approaches have mostly focused on the molecular dynamics of pore formation processes (Tieleman et al. 2003; Hu et al. 2005a, b; Vernier 2006a; Böckmann et al. 2008; Marrink et al. 2009). For numerical constraints, in most of these studies electric fields had to be applied that are orders of magnitude higher than used in actual experiments, and therefore a quantitative comparison with measurements is difficult. Accordingly, simulations in general fail to predict transmembrane voltages that are required for pores to form, and in fact often values such as 1 V are explicitly assumed as threshold criteria rather than derived (Gowrishankar et al. 2006; Vernier et al. 2006a). However, the studies have offered important insight into the structure of the cell membrane itself and the rearrangement of molecules when an electric field is applied (Hu et al. 2005a; Vernier et al. 2006a; Vernier and Ziegler 2007; Böckmann et al. 2008; Marrink et al. 2009). In some experiments these rearrangements have even been observed indirectly, for example, resulting in the externalization of phosphatidylserine after the application of 4 ns pulsed electric fields (Vernier et al. 2006b). We have recently reported on the first real-time measurements of transmembrane potential changes for cells exposed to nsPEFs (Frey et al. 2006). Changes in the fluorescence response of the voltage-sensitive, fast-response dye, Annine-6, were recorded with a temporal resolution of 5 ns. In this article, we present an extended study on changes in the charging of the outer membrane as the strength of the applied electric field is varied. A direct physiological effect of the electric field, although unlikely for the short-term exposure, was evaluated by the use of different ion channel blockers.

Materials and methods

Cell culture

Jurkat cells, a T-lymphocyte cell line, obtained from American Type Culture Collection (ATCC, Manassas, VA) were cultured in 75-cm^2 flasks in phenol red RPMI 1640 medium (Mediatech Cellgro, Herndon, VA) supplemented with 10% fetal bovine serum (Atlanta Biologicals, Norcross, GA), 1% L-glutamine, and 1% penicillin/streptomycin (Mediatech Cellgro, Herndon, VA), and incubated at 37°C with 5% CO_2. Cells in log-phase were removed from the culture and re-suspended in a physiological buffer prior to experimentation. The re-suspension solution for Jurkat cells, unless otherwise noted, contained in mM: NaCl 145; KCl 5; NaH_2PO_4 0.4; $MgSO_4$ 1; glucose 6; HEPES 5 (pH 7.4 with NaOH); $CaCl_2$ 1.5.

Cell staining

Cells were stained with the voltage-sensitive, fast-response dye, Annine-6 (Sensitive Dyes GbR, Germany), at a concentration of 16 μM as previously described by Frey et al. (2006).

Experimental setup

Cells were placed in the gap (1 cm in length, 100 μm in height and width) between two plane parallel stainless steel electrodes that were mounted on a standard microscope slide. A homogeneous electric field was generated in the gap by means of a Blumlein line pulse generator build from a coaxial cable (RG58). Using a fast MOSFET switch (DEI275, IXYS RF, Fort Collins, CO), a single 60-ns high-voltage pulse with a rise time of 5 ns could be applied to a matched load resistance of 100 Ω. The pulse generator was synchronized with a pulsed laser source (a combination of dye laser and Nd:YAG pumping laser, models PDL-2 and DCR-3, respectively, Quanta Ray, Mountain View, CA), providing a 5-ns excitation of the voltage-sensitive dye. Consequently cells could be illuminated and a voltage response recorded for different time points during and after the exposure to an electric field with a resolution of 5 ns with an open shutter camera. More details of the experimental setup can be found elsewhere (Frey et al. 2006).

Fluorescence microscopy and image analysis

Photographs of the Jurkat cells were taken on an inverted microscope (Olympus IX71, Melville, NY) with 600× magnification. A reference picture was taken before the electric field exposure and another during the application of the electric field. Images of the cells were recorded in 12-bit grayscale with a signal-amplifying camera (PCO DiCAM Pro, The Cooke Corp., Auburn Hills, MI). The images were processed with a program developed in MatLab (The MathWorks, Inc., Natick, MA). In each set of corresponding photographs, taken before and during the exposure, the cells were outlined with circular masks of radius r. The value of r varies with cell size but was kept the same for the same cell in corresponding photographs. Circles with a radius of 0.25r were placed on the cell perimeter at the pole facing the anode (3 o'clock) and the cathode (9 o'clock) at a distance of 0.75r from the center of the cell. After background intensities were subtracted, the relative average change in fluorescence pixel intensities $\Delta F/F_0$ ($\Delta F = F_e - F_0$, F_e: intensity during exposure, F_0: intensity before exposure) was calculated for the respective areas of interest. The relatively low standard error of our measurements is due to the time resolution of our experiments being sub-physiological and not necessarily dependent on the age or condition of the cell being analyzed.

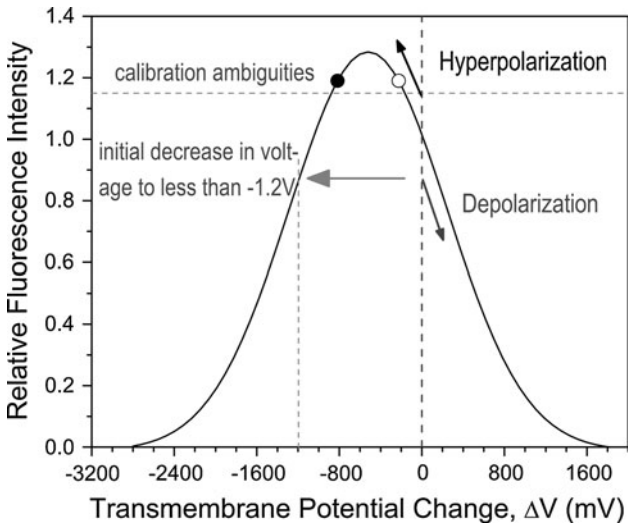

Fig. 1 Annine-6 calibration curve as determined by Kuhn and Fromherz (2003). For a decrease in the fluorescence signal, a transmembrane voltage change can be assigned for the depolarized and hyperpolarized hemisphere. However, relative changes of more than 100%, i.e., an increase in intensity, can be caused by two alternative voltages. An example is given by the *empty* and *filled circle* in the figure. Although the fluorescence intensity is the same for both data points, the corresponding voltage differs by approximately 600 mV

Voltage calibration

The fluorescent response of the voltage-sensitive dye Annine-6 has been studied in detail by Kuhn et al. (2004) and Kuhn and Fromherz (2003). For transmembrane voltage changes of ±300 mV, the shift of excitation and emission spectra has been measured and could be fitted with a semi-empirical relation. Based on the underlying mechanism of the response, it can be assumed that the analytical description can be extrapolated towards higher electric fields of up to 30 MV/cm, i.e., corresponding to transmembrane voltages of 30 V across a 10-nm-thick membrane (Fischer et al. 1976). For the excitation wavelength of 440 nm of our experiments, the calibration curve shown in Fig. 1 can be derived. The graph describes the relative change in the emission intensity depending on the voltage applied across the membrane, when observing the emission through a filter with a transmission between 560 and 660 nm, as was the case in our setup. A more detailed discussion of this calibration is given elsewhere (Frey et al. 2006).

Results

In order to analyze charging and discharge mechanisms of cell membranes exposed to nsPEFs, we stained Jurkat cells with the fast-response, voltage-sensitive dye, Annine-6. Pulsed electric fields of 60 ns were applied with different field strengths of 5, 12.5, 50, and 90 kV/cm. For each set of conditions, the development of fluorescence intensity was reconstructed from separate experiments where the change in fluorescence intensity was recorded at 5 ns intervals from 10 ns before the pulse was applied, throughout the pulse, and up to 240 ns after the pulse.

Assessment of fluorescence intensity changes

An example of the field-dependent response at a time of 15 ns into the exposure is shown in Fig. 2 for different field strengths. The change in the fluorescence intensity is of greater magnitude as higher electric field strengths are applied, indicating that a higher transmembrane voltage is reached. Notice that there is no obvious angular dependency along the cell membrane. The fluorescence intensity shows only a discontinuity at the equator (perpendicular to the direction of the electric field). As mentioned in our earlier publication this is the result of a uniform 'break down" of the membrane because of the high electric field strength that is applied. Consequently the transmembrane voltage is the same across hemispheres, although the value is different between the anodic and the cathodic side (Frey et al. 2006). For the applied field strengths presented here,

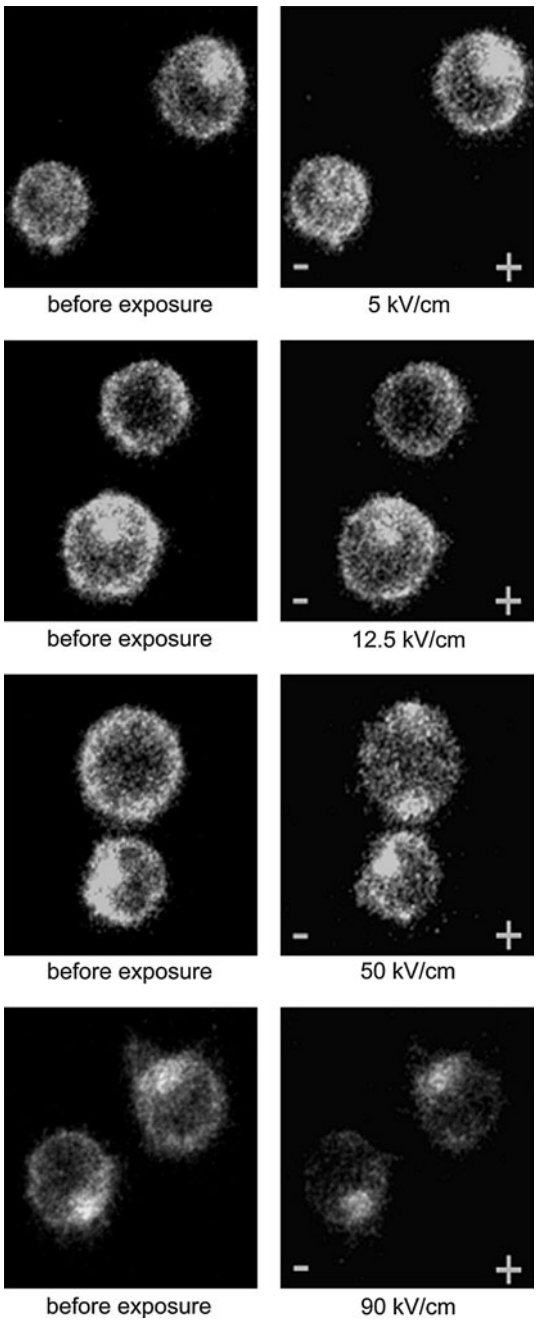

Fig. 2 Typical images of Annine-6-stained Jurkat cells taken 15 ns into a 90, 50, 12.5, or 5 kV/cm electric field pulse of 60-ns duration. The position of the electrodes is depicted with the anode to the right and the cathode to the left of each frame. Each *left* and *right* image pair is a unique experiment. For the same time during electric field application of 15 ns, stronger changes of the fluorescence emission are observed for higher field strengths. This corresponds to a higher transmembrane voltage change of the plasma membrane

the voltage at the anodic pole changes very fast, and moderate transient voltages that would correspond to an increase in fluorescence intensity could not be captured within the 5-ns resolution limit of our method. Instead, the observed immediate decrease of the fluorescence intensity at both poles of the cell indicates a fast rise in the transmembrane voltage with a change of more than 1 V occurring at the anodic pole.

Derivation of transmembrane voltage changes

The relative changes of the fluorescence signal for different times during exposure to electric fields of different strengths are shown in the left column of Fig. 3. The right column shows the transmembrane voltages that can be derived from the recorded fluorescence intensity change according to the calibration presented in Fig. 1. For measurements close to the maximum of the calibration curve, the analysis of the data provides ambiguous results. In the vicinity of this maximum (relative fluorescence intensity greater than 1.0), the fluorescence response can be attributed to two different voltages. Both possible values are shown in Fig. 3 by solid and open circles, respectively. The difference between alternative values can be as much as 1 V (Fig. 3) and is sensitive to small statistical errors.

After the initial sudden increase to 1 V, the potential differences at the anodic pole continue to rise at a more moderate rate to $\sim$1.6 V for applied field strengths equal to or greater than 50 kV/cm. Once this peak value is attained the transmembrane voltage begins to decrease, and it is notable that this instant drop in voltage occurs *while* the electric field is still being applied. This event suggests that a threshold voltage has been reached. The rate of change from the initial jump up to the peak values is approximately the same for both hemispheres of the cell. However, the maximum transmembrane voltages at the anode lie between 1.4 and 1.6 V and between 0.5 and 0.6 V for the cathode pole. For all applied field strengths the cathode pole values are generally 1 V lower than the voltages at the anode side. For the lower field strengths of 5 and 12.5 kV/cm, voltages remain near the peak, once attained, throughout the remaining pulse duration, and the distinct drop seen with application of higher field strengths is absent.

Initial membrane charging phase

With the calibration ambiguity in mind, it is important to notice that for every field strength the voltage is immediately exceeding 1 V at the anodic pole when an electric field is applied. For the higher electric fields of 50 and 90 kV/cm of our study, an increase in transmembrane voltage to more than 1 V can be expected within 5 ns or less, i.e., the resolution limit of our method, expected from basic membrane charging models, such as Schwan's equation (Schwan 1957; Schoenbach et al. 2004). However, the theory cannot explain the jump for lower field strengths of 5 and 12.5 kV/cm. A subsequent further

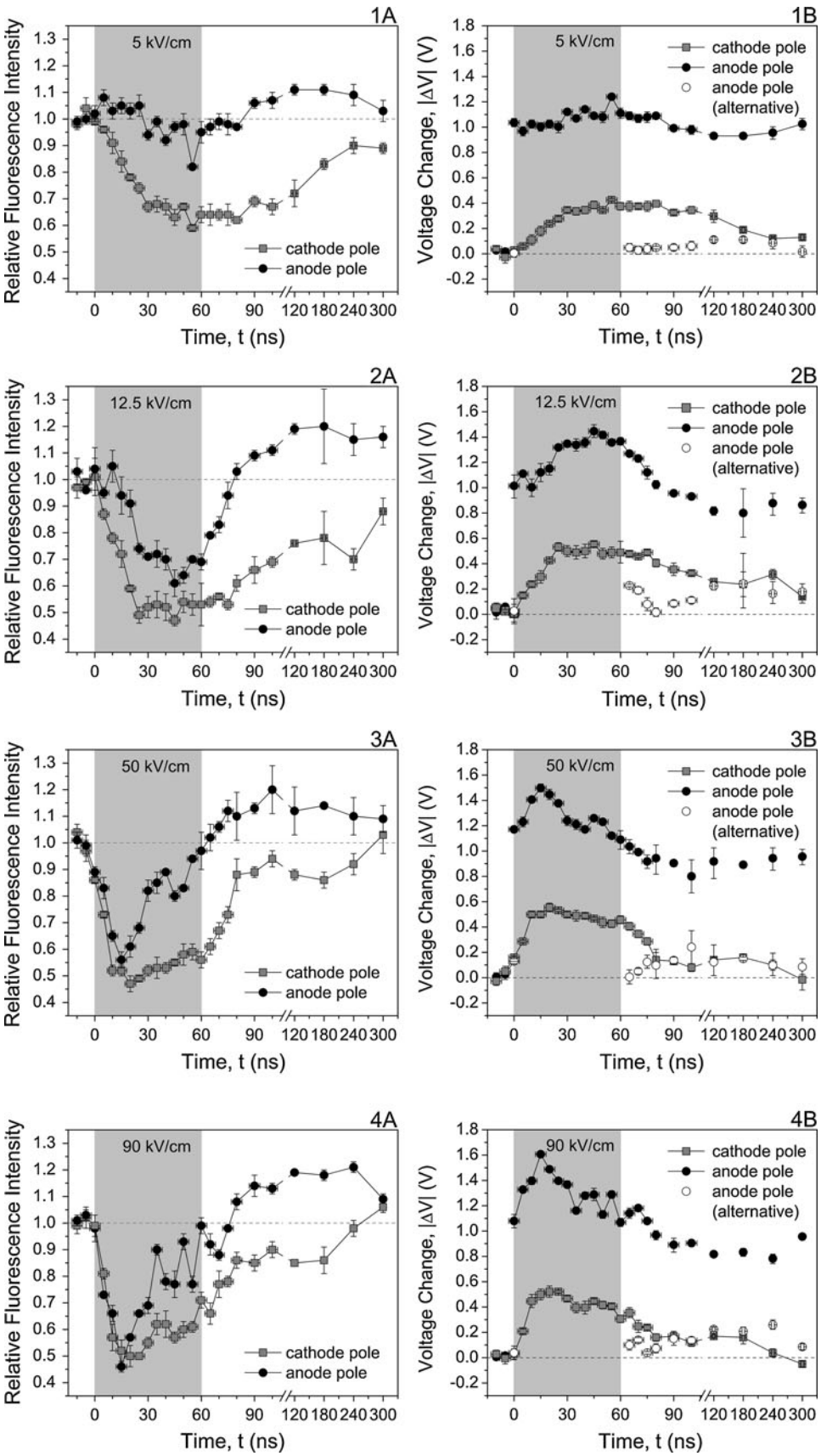

Fig. 3 Jurkat cells stained with the voltage-sensitive dye, Annine-6, show a change in relative fluorescence intensity (*left column*) in response to nsPEF treatment. The change in fluorescence intensity reflects a change in transmembrane potential (*right column*). Each pair, i.e., **1a** and **1b**, represents the relative fluorescence intensity and transmembrane potential data for one electric field. The electric fields that were applied are as follows: (1) 5, (2) 12.5, (3) 50, and (4) 90 kV/cm. The *shaded area* depicts the time when the 60-ns duration electric field was applied. Alternative voltage values are presented as *open circles*. Average values represent an n of 5 ± SE bars

increase in transmembrane voltage is qualitatively consistent with the conductive charging models for all applied electric fields, but with charging time constants that are about six times longer than expected for an ideal insulating membrane. Without the indicative rise to a peak value, voltages obtained for the lowest investigated field strength of 5 kV/cm have to be interpreted very careful. In this case, it seems only warranted for later times during the exposure to assign values of about 1.1 V to the membrane potential change. Conversely, this result suggests that voltage changes due to a contribution from charging currents are rather small compared to the initial dielectric effects, which likely lead to the immediate jump in voltage to more than 1 V. Only eventually will the charging currents then shift the voltage toward slightly higher and unambiguous values.

Discharge phase

Once the external electric field is removed, the resting transmembrane voltage starts to decrease again towards resting values. The ambiguities of the calibration for these smaller voltages do not allow us to determine the time constants of this decay exactly. The 5 kV/cm field strength effects are difficult to interpret since it appears that the voltage remains elevated long after the pulse application has ended. It is also worth mentioning that because of restrictions of our experimental setup, an electric field with 20% of the strength of the initial applied field remains for another 60 ns after the pulse. This may contribute to the residual elevated transmembrane voltages seen after the pulse.

Effect of channel blockers

Although the change in membrane potential was not expected to be biological in nature because of the ultra-fast time scale, verification that it was a sub-physiological response was tested by measuring the response of the cells to a 60-ns pulsed electric field of 90 kV/cm in the presence of several common ion channel blockers and also the use of a sodium-substituted buffer solution with glucamine. TEA, lanthanum, verapamil, nifedipine, diltiazem, TTX, and a sodium-substituted glucamine medium were each evaluated separately for their effect on the response of the cells to nsPEF-induced changes in transmembrane potential. (All chemicals, except for diltiazem, were obtained from Sigma-Aldrich, St. Louis, MO. Dilitiazem was obtained from Marion Laboratories, Kansas City, MO.) The results are shown in Table 1.

Only the use of TTX, a voltage-gated sodium channel blocker, resulted in a transmembrane voltage change slightly higher than without (1.7 V instead of 1.6 V), but only at the anodic pole. The use of glucamine-substituted media decreased the degree of change of transmembrane voltage change at both the anode and cathode poles to 1.5 and 0.55 V, respectively (instead of 1.6 and 0.5 V). All observed differences fall within an error range of 3 standard deviation and are therefore at least on this level not statistically significant. Thus, we feel that the response in transmembrane potential is most likely sub-physiological.

Discussion

A number of studies on the biological effects of nsPEF have suggested a dependency of the onset of cellular responses on the product of pulse duration and field strength (Beebe et al. 2003; Pakhomov et al. 2004; Zhang et al. 2008; Scarlett et al. 2009; Nuccitelli et al. 2009). On one hand, a threshold can be defined by this convention, which, when achieved, will induce a specific response of the cell such as apoptosis (Beebe et al. 2003). On the other hand, the primary physical processes, which are determined by the product of field strength and pulse duration, are electrically charging mechanisms. Consequently, a direct threshold effect in the transmembrane voltage of the plasma membrane is expected, which can be related to the observed biological responses. For very fast transients on the order of 1 ns, dielectric effects will dominate the charging process, as can be seen by the immediate rise of transmembrane voltages as soon as the electric field is applied. To study the charging of the cell membrane for different conditions, we have developed a diagnostic method that allows measurements of transmembrane voltage changes in real-time, i.e., with a temporal resolution much shorter than the duration of the applied pulse.

Pore formation threshold

Our experiments support the hypothesis of a membrane charging threshold related to a biological response. To instigate a lasting physiological response, it seems necessary to reach a transmembrane voltage of 1.4–1.6 V across the anodic hemisphere. Further development then likely depends on the rate of pore formation if the electric field is applied for a long time after this threshold level is reached.

The peak values observed in our experiments are much lower than was expected from passive membrane models, which assume for short pulse exposures only dielectric charging mechanisms (Deng 2003; Vernier et al. 2004a; Kotnik and Miklavcic 2006). Conversely, the intriguing fit of the results with active models suggests that the formation of pores can be expected early on and will determine the continuing charging of the membrane more and more (Hu et al. 2005a; Smith and Weaver 2008).

Table 1 Maximum transmembrane potential change, $|\Delta V_{anode,max}|$, for the anodic and maximum transmembrane potential change, $|\Delta V_{cathode,max}|$, cathodic pole, for an exposure to a 60-ns, 90 kV/cm electric field when different ion channel blockers were added to the cell suspension

Channel blocker	Concentration	$\lvert\Delta V_{anode,max}\rvert$ (V)	$\lvert\Delta V_{cathode,max}\rvert$ (V)
No channel blocker (control)	–	1.60	0.65
Tetraethyl ammonium chloride	30 mM	1.52	0.60
Diltiazem HCl	200 μM	1.60	0.62
Nifedipine	200 μM	1.58	0.61
Verapamil HCl	200 μM	1.61	0.61
Lanthanum chloride	1 mM	1.58	0.60
N-Methylglucamine chloride	150 mM	1.50	0.55
Tetrodotoxin	1 μM	1.70	0.65

Effect of head group dipole alignments on measurements

Remarkably, the voltage across the cathodic pole is generally 1 V less than across the anodic pole. Two main mechanisms could contribute to this difference in transmembrane voltages: First, local perturbations in electric fields occur at the site of Annine-6 molecules embedded in the outer leaflet by the reorientation of lipid polar head groups by the applied electric field. A strong effect on the orientation of lipid headgroups was also confirmed in molecular simulation studies (Vernier 2006a; Böckmann et al. 2008; Marrink et al. 2009). These studies further showed that strong intrinsic field gradients on the order of the applied electric fields are found in the head group regions of the lipid bilayer in its resting state. An applied electric field was shown to result in a strong asymmetry across these interface regions on both sides of the bilayer. Since the molecules of the voltage-sensitive dye are only embedded on the outer leaflet, the asymmetry transposes accordingly to differences in the response at the anodic and the cathodic pole, which will in return affect the fluorescence as given by the shift of excitation and emission spectra in an electric field. Without an electric field applied, these head groups are generally oriented (more or less) perpendicular to the membrane surface. Thermal motion, however, causes random deviations and fluctuations in the angle of the polarization vector as depicted in Fig. 4a. Since the quasi-negative charge of the head group dipole is closer to the lipid tail for almost all phospholipids, the polarization vector is generally pointing away from this tail when no electric field is applied. In a strong enough electric field, the dipoles will start to turn in the direction of this external field. The rotation occurs primarily at the outer anodic leaflet (and the inner leaflet at the cathode pole), though it is somewhat impeded by the torque imposed by the fatty acid tail anchor of the phospholipids (Fig. 4b). As a result of the dipole re-alignment, the local electric field will change, as the localized polarization (i.e., the screening ability) changes. This rapid dipole reorientation, which is expected to occur almost immediately, i.e., on a time scale of about 1 ns, when the electric field is applied, will change the local electric fields in the outer leaflet of the bilayer *between* the head groups of the phospholipids. At the anode pole the dipole screening weakens, whereas at the cathode pole the small and random changes in dipole orientation will not lead to a significant perturbation in the shielding of the applied electric field. Since the dye molecules of Annine-6 are embedded between the phospholipid head groups of the outer leaflet, their fluorescence response is determined by these local electric fields (externally applied less the dipole screening) as can be described by the molecular Stark effect. Notice that this dielectric effect, responsible for the voltage asymmetry between the anode and cathode pole, does not require poration since the dipole swing is a fast "pre-poration" event that creates local "defects" that can eventually lead to a pore. Hence, it is understandable, because of this fast process, that the measured voltage change at the anode, in particular for exposures to 5 and 12.5 kV/cm, increases to more than 1 V almost instantaneously when an electric field is applied and immediately instigates the formation of pores. In addition, since the reorientation of the head group dipoles will be the same, independent of their location on each hemisphere of the cell, an angular dependency of changes in fluorescence intensity is not expected. However, a distinct jump from one value to the other along the cell equator (perpendicular to the applied electric field) is observed in our experiments (Fig. 2). Moreover the contributions of this dipole effect to the voltage difference across the membrane will last as long as an electric field of sufficient strength is applied.

Effect of membrane poration events on transmembrane voltage development

Eventually charging mechanisms by ion currents will contribute more and more to the potential difference across the membrane and lead to a further increase in transmembrane voltage above the values determined by this

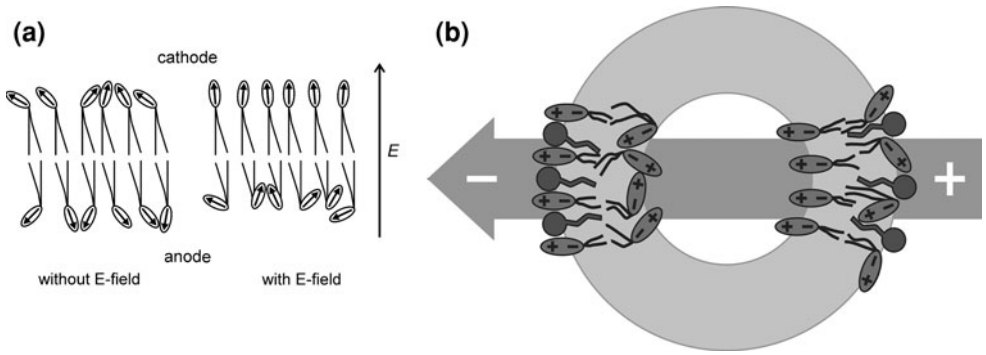

Fig. 4 **a** cartoon depicting neutral lipid molecules, which form the plasma membrane, under the influence of an applied electric field; **b** transmembrane voltage asymmetry upon field application. Head group dipoles of phospholipids are immediately aligned upon application of a strong electric field. This leads to a decrease of the local electric field strength at the location of dye molecules in the outer leaflet at the cathode pole and to an increase at the anode pole, respectively. This local field determines the fluorescence response

dipole effect. For a transmembrane voltage of more than 1 V, the formation of pores is expected. As a result pores might start to form at the anode pole immediately and in effect provide leakage pathways that will slow down further charging of the membrane. For this case a more random orientation of head groups on the anode side might also facilitate pore formation, whereas at the cathode tighter packing hampers the process. Benz has found pore formation times of less than 10 ns for the application of microsecond pulses (Benz and Zimmermann 1980). Experiments by Vernier and computer simulations suggest pore formation times that are even shorter for the application of nanosecond pulses (Vernier et al. 2006a; Hu et al. 2005a). Therefore, the actual onset of pore formation may actually be—for the moment—outside the reach of our diagnostic capabilities. According to the observed drop in voltage, after reaching peak voltages of 1.4–1.6 V, these mechanisms are eventually becoming dominant and will enable high ion currents across this barrier, leading to a decrease in voltage even while the electric field is still applied. The creation of pores can also explain the asymmetrical charging *and* discharge response, especially for the higher electric field strengths of 50 and 90 kV/cm. Several studies show that pores created at the cathode pole are in general larger (Tekle et al. 1990; Lojewska et al. 1989; Tekle et al. 2001; Tarek 2004; Escoffre et al. 2009). In addition the lateral transport of negatively charged phosphatidylserine molecules towards or away from pores, depending at which pole the pores have formed, will either impede or promote the migration of ions through the pores (Hu et al. 2005a). The continuing increase in transmembrane potential up to values of 1.6 V at the anodic pole and 0.6 V at the cathodic side implies that during the rise to this value, the charging rate is greater than the ion exchange rate through the created pores. A suggested directionality for the transport of ions through a pore with respect to the direction of the applied electric field may furthermore contribute to the observed asymmetry in membrane potentials at opposite poles (Hu et al. 2006).

Experimental challenges in the data interpretation

The aforementioned ambiguities in the calibration of data for transmembrane voltages at the anode of 800 mV or less result in a difficult interpretation for measurements after the end of the 60-ns exposure when voltages continue to decrease. We consequently present both possible values of the transmembrane voltages at the anodic pole in Fig. 3 by open and solid circles, respectively.

The development of the transmembrane voltages in particular at the anodic pole is strongly affected by the residual electric field after the first 60 ns of the exposure. During this post-exposure a field of still 20% of the strength of the initially applied pulse is likely to sustain the orientation of head groups for another 60 ns. Especially for the higher applied fields of 90 and 50 kV/cm, the field during this second phase is comparable to the applied field of 5 kV/cm. This is sufficient to maintain a transmembrane voltage of about 1 V at the anodic pole, although ion currents are already discharging the membrane. As soon as the field approaches zero, the orientation of the head groups will become random, accompanied by an almost sudden drop in transmembrane voltage. From this time on, the measured values represent only the potential difference due to the remaining ion imbalance across the membrane. The loss of the orderly state of the dipole moments in the outer leaflet of the membrane at the anodic pole is determined by the energy threshold determined by the Brownian motion of the molecules. For lower field strengths of 5 and 12.5 kV/cm, the energy provided by the reduced electric field in the post-exposure phase is falling below this threshold faster, and accordingly we anticipate that the transmembrane voltage "jumps" down to lower values earlier. Unfortunately our current setup does not allow us to

resolve this transition. It will require an improved pulse delivery system, which eliminates the residual electric field, and increasing the dynamic response of the diagnostic for smaller transmembrane voltages, for example, by a different excitation.

Pore formation development

As long as dipole contributions to the local electric field in the membrane are high, they camouflage the discharge of the membrane through conductive ion currents. When only a few or only small pores are formed during the exposure, the membrane can only discharge slowly with a time constant identical to the charging time constant on the order of 100 ns (Schoenbach et al. 2001). This is the case for the lowest electric fields in our study. For exposure to 5 kV/cm, the threshold value of 1.4–1.6 V that seems to indicate the onset of significant pore formation is not reached at all and for 12.5 kV/cm only towards the very end of the applied pulse. Accordingly the transmembrane voltage is not changing until the dipole orientation of lipid head groups is lost up to 120 ns after the pulse at most. A faster conductive discharge after the pulse is, however, expected for higher electric fields when the threshold for membrane permeabilization is reached early during exposure, providing an additional discharge pathway (Marrink et al. 2009). So far, no direct experimental evidence for the proposed formation of small pores could be found. Traditional membrane integrity markers such as propidium iodide and ethidium homodimer are not permeable until several minutes after exposure (Beebe et al. 2003; Chen et al. 2004). The uptake is therefore considered a secondary response as these dyes pass through large pores that open later as a physiological response of the cell to the stimulation. From this experiment it is also apparent that the size of primary pores in the membrane, which are formed during the pulse and are responsible for conduction across the membrane, must be much smaller than the size of traditional membrane integrity molecules with a diameter suggested to be on the order of 1 nm (Gowrishankar et al. 2006; Bowman et al. 2010).

Biological response to nanosecond pulsed electric field exposures

Because the fastest biological response time is on the order of milliseconds, the observed changes in transmembrane potential cannot be explained by a physiological response. This is confirmed by our control experiments with ion channel blockers. All measurements showed almost no effect of the blockers or substituted media on the membrane potential response to nsPEF. The measurements conducted during the exposure, however, do not exclude the possibility that physiological pathways will have been altered by the electric field. In fact, it is very likely that these pathways are significantly influenced by nsPEF stimulation (Beebe and Schoenbach 2005), although an effect on membrane protein function is not expected to occur on a nanosecond time scale.

In closing, comparing the conditions that enable a cell to reach the threshold value for a sustained membrane poration to those reported to induce apoptosis suggests that the pulse parameters for electric field and pulse duration are similar (Beebe et al. 2003). Within the range of electric fields that are used in this study other work has shown that release of intracellular calcium, caspase activation, and phosphatidyl serine exposure can be attributed to nsPEF effects (White et al. 2004; Beebe et al. 2003). We theorize that it is the initial plasma membrane or intracellular membrane effects on a nanosecond time scale that cause other signaling cascades (in the second to minute time scale) to be activated. The observed limits in transmembrane voltages, which are only slightly dependent on the field strength for higher electric fields, show that when the membrane is breached, subcellular structures are exposed to electric fields that are of similar magnitude to the applied electric field. Consequently, membrane effects similar to what we observe for the plasma membrane are expected and anticipated for intracellular membranes possibly interfering with cell signaling pathways (Beebe and Schoenbach 2005; White et al. 2004; Scarlett et al. 2009). Further studies are necessary to substantiate this hypothesis derived from the limited number of data available for different exposure conditions. If this relationship can be established, it will be possible to predict the conditions that are necessary to induce apoptosis. Based on this information treatments can be designed that aim at the selective removal of cells, in particular cancer cells.

Acknowledgments This study was funded by an AFOSR DOD MURI grant on "Subcellular Response to Narrow Band and Wide Band Radio Frequency Radiation" administered by Old Dominion University. We would also like to thank Peter Fromherz (Max Planck Institute for Biochemistry) and Bernd Kuhn (Max Planck Institute for Medical Research) for their valuable advice and assistance in discussions regarding the Annine-6 dye.

References

Beebe SJ, Schoenbach KH (2005) Nanosecond pulsed electric fields: a new stimulus to activate intracellular signaling. J Biomed Biotechnol 4:297–300. doi:10.1155/JBB.2005.297

Beebe SJ, Fox PM, Rec LJ, Willis EL, Schoenbach KH (2003) Nanosecond, high-intensity pulsed electric fields induce apoptosis in human cells. FASEB J 17:1493–1495. doi:10.1096/fj.02-0859fje

Beebe SJ, White J, Blackmore PF, Deng Y, Somers K, Schoenbach KH (2004a) Diverse effects of nanosecond pulsed electric fields

on cells and tissues. DNA Cell Biol 22:785–796. doi:10.1089/104454903322624993

Beebe SJ, Blackmore PF, White J, Joshi RP, Schoenbach KH (2004b) Nanosecond pulsed electric fields modulate cell function through intracellular signal transduction mechanisms. Physiol Meas 25:1077–1109. doi:10.1088/0967-3334/25/4/023

Benz R, Zimmermann U (1980) Pulse lenght dependence of the electrical breakdown in lipid bilayer membranes. Biochim Biophys Acta 597:637–642

Böckmann RA, de Groot BL, Kakorin S, Neumann E, Grubmüller H (2008) Kinetics, statistics, and energetics of lipid membrane electroporation studied by molecular dynamics simulations. Biophys J 95:1837–1850. doi:10.1529/biophysj.108.129437

Bowman AM, Nesin OM, Pakhomova ON, Pakhomov AG (2010) Analysis of plasma membrane integrity by fluorescent detection of Tl^+ uptake. J Membrane Biol 236:15–26. doi:10.1007/s00232-010-9269-y

Chen N, Schoenbach KH, Kolb JF, Swanson RJ, Garner AL, Yang J, Joshi RP, Beebe SJ (2004) Leukemic cell intracellular responses to nanosecond electric fields. Biochem Biophys Res Commun 317:421–427. doi:10.1016/j.bbrc.2004.03.063

Deng J, Schoenbach KH, Buescher ES, Hair PS, Fox PM, Beebe SJ (2003) The effects of intense submicrosecond electrical pulses on cells. Biophys J 84:2709–2714. doi:10.1016/S0006-3495(03)75076-0

Escoffre J-M, Portet T, Wasungu L, Teissié J, Dean D, Rols M-P (2009) What is (still not) known of the mechanism by which electroporation mediates gene transfer and expression in cells and tissues. Mol Biotechnol 41:286–295. doi:10.1007/s12033-008-9121-0

Fischer JK, von Bruning DM, Labhart H (1976) Lightmodulation by electrochromism. Appl Opt 15:2812–2816

Frey W, White JA, Price RO, Blackmore PF, Joshi RP, Nuccitelli RL, Beebe SJ, Schoenbach KH, Kolb JF (2006) Plasma membrane voltage changes during nanosecond pulsed electric field exposure. Biophys J 90:3608–3615. doi:10.1529/biophysj.105.072777

Gowrishankar TR, Esser AT, Vasilkoski Z, Smith KC, Weaver JC (2006) Microdosimetry for conventional and supra-electroporation in cells with organelles. Biochem Biophys Res Commun 341:1266–1276. doi:10.1016/j.bbrc.2006.01.094

Hu Q, Joshi RP, Schoenbach KH (2005a) Simulations of nanopore formation and phosphatidylserine externalization in lipid membranes subjected to a high-intensity, ultrashort electric pulse. Phys Rev E 72:031902(10 pp). doi:10.1103/PhysRevE.72.031902

Hu Q, Viswanadham S, Joshi RP, Schoenbach KH, Beebe SJ, Blackmore PF (2005b) Simulations of transient membrane behavior in cells subjected to a high-intensity ultrashort electric pulse. Phys Rev E 71:031914. doi:10.1103/PhysRevE.71.031914

Hu Q, Sridhara V, Joshi RP, Kolb JF, Schoenbach KH (2006) Molecular dynamics analysis of high electric pulse effects on bilayer membranes containing DPCC and DPSS. IEEE Trans Plasma Sci 34:1405–1411. doi:10.1109/TPS.2006.876501

Joshi RP, Hu Q, Schoenbach KH (2004) Modeling studies of cell response to ultrashort, high-intensity electric fields–implications for intracellular manipulation. IEEE Trans Plasma Sci 32:1677–1688. doi:10.1109/TPS.2004.830971

Knisley SB, Blitchington TF, Hill BC, Grant AO, Smith WM, Pilkington TC, Ideker RE (1993) Optical measurements of transmembrane potential changes during electric field stimulation of ventricular cells. Circ Res 72:255–270

Kotnik T, Miklavcic D (2006) Theoretical evaluation of voltage inducement on internal embranes of biological cells exposed to electric fields. Biophys J 90:480–491

Krassowska W, Neu JC (1994) Response of a single cell to an external electric field. Biohpys J 66:1768–1776. doi:10.1016/S0006-3495(94)80971-3

Kuhn B, Fromherz P (2003) Annellated hemicyanine dyes in a neuron membrane: molecular stark effect and optical voltage recording. J Phys Chem B 107:7903–7913

Kuhn B, Fromherz F, Denk W (2004) High sensitivity of Stark-shift voltage-sensing dyes by one- or two-photon excitation near the red spectral edge. Biophys J 87:631–639. doi:10.1529/biophysj.104.040477

Lojewska Z, Farkas DL, Ehrenberg B, Loew LM (1989) Analysis of the effect of medium and membrane conductance on the amplitude and kinetics of membrane potentials induced by externally applied electric fields. Biophys J 56:121–128. doi:10.1016/S0006-3495(89)82657-8

Marrink JS, de Vries Tieleman DP AH, Tieleman DP (2009) Lipids on the move: simulations of membrane pores, domains, stalks and curves. Biochim Biophys Acta 1788:149–168. doi:10.1016/j.bbamem.2008.10.006

Nuccitelli R, Pliquett U, Chen X, Ford W, Swanson RJ, Beebe SJ, Kolb JF, Schoenbach KH (2006) Nanosecond pulsed electric fields cause melanomas to self-destruct. Biochem Biophys Res Commun 343:351–360. doi:10.1016/j.bbrc.2006.02.181

Nuccitelli R, Chen X, Pakhomov AG, Baldwin WH, Sheikh S, Pomicter JL, Ren W, Osgood C, Swanson RJ, Kolb JF, Beebe SJ, Schoenbach KH (2009) A new pulsed electric field therapy for melanoma disrupts the tumor's blood supply and causes complete remission without recurrence. Int J Cancer 125:438–445. doi:10.1002/ijc.24345

Pakhomov AG, Phinney A, Ashmore J, Walker K III, Kolb JF, Kono S, Schoenbach KH, Murphey MR (2004) Characterization of the cytotoxic effect of high-intensity, 10 ns duration electrical pulses. IEEE Trans Plasma Sci 32:1579–1586. doi:10.1109/TPS.2004.831773

Scarlett SS, White JA, Blackmore PF, Schoenbach KH, Kolb JF (2009) Regulation of intracellular calcium concentrations by nanosecond pulsed electric fields. Biochim Biophys Acta 1788:1168–1175. doi:10.1016/j.bbamem.2009.02.006

Schoenbach KH, Beebe SJ, Buescher ES (2001) Intracellular effect of ultrashort electrical pulses. Bioelectromagnetics 22:440–448. doi:10.1002/bem.71

Schoenbach KH, Joshi RP, Kolb JF, Chen N, Stacey M, Blackmore PF, Buescher ES, Beebe SJ (2004) Ultrashort electrical pulses open a new gateway into biological cells. Proc IEEE 90:1122–1137. doi:10.1109/JPROC.2004.829009

Schwan HP (1957) Electrical properties of tissue and cell suspension. Adv Biol Med Phys 5:147–209

Simcic S, Bobanovic F, Kotnik V, Vodovnik L (1997) Local changes in membrane potential intensify neutrophil oxidative burst. Phsiol. Chem Phys Med NMR 29:39–50

Smith KC, Weaver JC (2008) Active mechanisms are needed to describe cell responses to submicrosecond, megavolt-per-meter pulses: cell models for ultrashort pulses. Biophys J 95:1547–1563. doi:10.1529/biophysj.107.121921

Tarek M (2004) Membrane electroporation: a molecular dynamics simulation. Biophys J 88:4045–4053. doi:10.1529/biophysj.104.050617

Teissié J, Eynard N, Vernhes MC, Benichou A, Ganeva V, Galutzov B, Cabanes PA (2002a) Recent biotechnological developments of electropulsation. A prospective review. Bioelectrochemistry 55:107–112. doi:10.1016/S1567-5394(01)00138-4

Teissié J, Golzio M, Rols MP (2002b) Mechanisms of cell membrane electropermeabilization: a minireview of our present (lack of?) knowledge. Biochim Biophys Acta 1724:270–280. doi:10.1016/j.bbagen.2005.05.006

Tekle E, Astumian RD, Chock PB (1990) Electro-permeabilization of cell membranes: effect of the resting membrane potential. Biochem Biophys Res Commun 172:282–287

Tekle E, Astumian RD, Friauf WA, Chock PB (2001) Asymmetric pore distribution and loss of membrane lipid in electroporated DOPC vesicles. Biophys J 91:960–968. doi:10.1016/S0006-3495(01)75754-2

Tieleman DP, Leontiadou H, Mark AE, Marrink S-J (2003) Simulation of pore formation in lipid bilayers by mechanical stress and electric fields. J Am Chem Soc 125:6382–6383. doi:10.1021/ja029504i

Tsong TY (1991) Electroporation of cell membranes. Biophys J 60:297–306. doi:10.1016/S0006-3495(91)82054-9

Vernier PT, Ziegler MJ (2007) Nanosecond field alignment of head group and water dipoes in electroporating phospholipid bilayers. J Phys Chem B 111:12993–12996. doi:0.1021/jp077148q

Vernier PT, Sun Y, Marcu L, Craft CM, Gundersen MA (2004a) Nanoelectropulse-induced phosphatidylserine translocation. Biophys J 86:4040–4048. doi:10.1529/biophysj.103.037945

Vernier PT, Sun Y, Marcu L, Craft CM, Gundersen MA (2004b) Nanosecond pulsed electric fields perturb membrane phospholipids in T lymphoblasts. FEBS Letters 572:103–108. doi:10.1016/j.febslet.2004.07.021

Vernier PT, Ziegler MJ, Sun Y, Gundersen MA, Tieleman DP (2006a) Nanopore-facilitated, voltage-driven phosphatidylserine translocation in lipd bilayers–in cells and in silicio. Phys Biol 3:233–247. doi:10.1088/1478-3975/3/4/001

Vernier PT, Sun Y, Gundersen MA (2006b) Nanoelectropulse-driven membrane perturbation and small molecule permeabilization. BMC Cell Biology 7:37. doi:10.1186/1471-2121-7-37

White JA, Blackmore PF, Schoenbach KH, Beebe SJ (2004) Stimulation of capacitative calcium entry in HL-60 cells by nanosecond pulsed electric fields. J Biol Chem 279:22964–22972

Zhang J, Blackmore PF, Hargrave BY, Xiao S, Beebe SJ, Schoenbach KH (2008) The characteristics of nanosecond pulsed electrical field stimulation on platelet aggregation in vitro. Arch Biochem Biophys 471:240–248